Turk J Engin Environ Sci
24 (2000) , 71 – 80.

Manufacturing and Testing of a V-Type Stirling Engine

Halit KARABULUT
Gazi University, Technical Education Faculty,
Mechanical Education Department,
06500, Beşevler, Ankara-TURKEY
Hüseyin Serdar YÜCESU, Atilla KOCA
Zonguldak Karaelmas University,
Karabük Technical Education Faculty,
Mechanical Education Department, 78100 Karabük-TURKEY

Received 06.11.1998

Abstract

An air charged V-type Stirling engine, having 260 cm^3 swept volume, was manufactured and tested. Speed-torque characteristics of the engine were obtained for different temperature and charge pressure values in the range of 600°C to 1100°C and 1 to 4 bars. The experiments intended to determine the performance characteristics of the engine at different set up values of pressure and hot source temperature. Maximum output power was obtained at 1100°C and 2.5 bars charge pressure as 65 W. The results are presented in diagrams.

Key Words: Stirling engine, external heating, engine performance, experimental study.

V Tipi Bir Stirling Motorunun İmalatı ve Testleri

Özet

Çalışma maddesi hava olan, 260 cm^3 süpürme hacmine sahip V tipi bir Stirling motoru imal edilmiş ve testleri yapılmıştır. Motor 600 °C-1100 °C sıcaklık ve 1-4 bar basınç sınırları arasında test edilerek hız-moment eğrileri elde edilmiştir. Deneyler motorun farklı şarj basınçlarında ve farklı sıcak kaynak sıcaklıklarında performans karakteristiklerini elde etmeyi amaçlamıştır. Motorun maksimum gücü, 1100 °C ısıtıcı sıcaklığı ve 2.5 bar şarj basıncında 65 W olarak elde edilmiştir. Sonuçlar grafik olarak sunulmuştur.

Anahtar Sözcükler: Anahtar kelimeler: Stirling motoru, dıştan ısıtma, motor performansı, deneysel çalışma.

Introduction

Stirling engines are externally heated, closed-cycle regenerative machines. Theoretical thermodynamic analysis of Stirling cycle engines indicates a thermal efficiency equal to that of the Carnot cycle. Although invented before Internal Combustion Engines, Stirling engines are not yet commercial today. The main reason preventing the Stirling engine from being commercial is its incompetetiveness with Internal Combustion Engines in specific power and weight (Walker, 1981; Rix, 1996).

After inventing the Stirling engine in 1816, Robert Stirling carried out investigations up to the

1850's and built double and triple cylinder engines, which were different in construction from the first engine. However, the performance of these engines was no better than that of the first engine. In 1860, Lehman built a horizontal single cylinder, displacer-piston type Stirling engine without regenerator. This engine was found to be more popular than the regenerative engines built by Stirling (Finkelstein, 1959a; Finkelstein, 1959b). In 1876, Rider used a novel construction on which expansion and compression spaces were set in different cylinders. On this engine, cylinders were side by side and externally connected to each other by a regenerator. The superiority of this engine was the simple maintenance and silent operation as a result of having only five moving parts. Up to 1915, the only progress made on Stirling engines was the rearrangement of cylinders at right angles to each other by Robinson. The best Stirling engine manufactured by the end of 1923 had about 800 kg mass and 1.5 kW power output and 3% thermal efficiency (Finkelstein, 1959b; Urieli and Rallis, 1975).

In 1938, Professor Holst noticed that there is a tremendous difference between the theoretical and practical thermal efficiency of Stirling engines. Professor Holst found this situation promising in consideration of the developments in material technology, and research was started again in the Physical Research Laboratories in Eindhoven under the direction of H. Rinia. Several successful prototypes were built that were 50 times lighter in weight and 125 times smaller in volume than the engine designed in 1923. The results of their researches were published in 1947. These engines, called Philips Stirling Engines, worked under 20-50 bar charge pressure and had a maximum speed of 2000-rpm and an output of 2 HP (Urieli and Rallis, 1975; Finkelstein, 1959c).

In 1953, a new driving mechanism was invented by R. J. Meijer in Philips-Eindhoven, the Rhombic Drive Mechanism (Meijer, 1960). The primary advantage of this engine was that the piston applies no force to the cylinder wall and allows the use of a flexible seal between the piston and cylinder wall. Consequently, no charge pressure is needed in the crankcase. R. J. Meijer used hydrogen, helium and air as working gas and obtained the best performance with hydrogen, the highest performance obtained up to that time (Michels, 1976).

After 1960, some engine companies (MAN-MWM, United Stirling of Sweden, Ford Motor Company of Detroit etc.) started research programs to develop Stirling engines for automotive applications. Within these programs some multi-cylinder engines having different driving mechanisms were built and tested. The thermal efficiency of Stirling engines designed for automotive application is over 40%. However, the weights and volumes are not at desired levels (Walker, 1981).

In 1974, W. Beale invented the free-piston Stirling engine. In this engine, the phasing between working piston and displacer is not realised by a driving mechanism. Therefore the engine has lower volume and weight, and thus has several advantages (Beale et. al., 1973). Particularly in solar energy research, it is appropriate to place the engine at the focus of a solar collector.

The practical cycle of Stirling engines differs from the theoretical cycle consisting of two constant temperatures and two constant volume processes. For the thermodynamic analysis of Stirling engines, more authentic approximations were devised. Schmidt (1871) introduced one of the approximations with the assumption that the fluids in hot and cold spaces are at the same temperature as the hot and cold sources respectively. In this analysis instead of theoretical processes, the real processes realised by pistons moving sinusoidally with 90-degrees phase angle are used. Another thermodynamic analysis was devised by Finkelstein (1967), called nodal analysis, wherein the whole engine was divided into 13 subvolumes. During the analysis at a cycle, the temperatures at subvolumes are calculated with differential time intervals by the First Law of Thermodynamics. In the analysis, the instantaneous variations of the wall temperatures are also taken into account. Urieli et al. (Urieli and Berchowitz, 1984; Urieli and Kushnir, 1982) improved the nodal analysis to cover the effects of leakage, heat losses and flow losses. Tew et al. (1978) conducted an investigation on nodal analysis, prepared computer programs and applied the design of a rhombic driven engine for NASA. The details of nodal analysis can be found in their report.

In the present study, a V-type Stirling engine prototype was designed and manufactured for solar energy and domestic applications.

Test Engine

The schematic view of the experimental engine is shown in Figure 1. The assembly of the crankshaft, piston rods and pistons is shown in Figure 2, and the

whole engine is shown in Figure 3. Essentially, the engine consists of a crankcase with two cylinders situated at 90° angles to each other, two cylinder-liners, a crankshaft beared from one end to the crank case, two connecting rods, two pistons both connected to the same crank journal, a regenerator and a connection pipe with a check-valve.

The wet type cylinder-liners were made of AISI 4080 SPECIAL steel. Pistons were made of Sphero cast iron, which includes graphite and does not require steady lubrication. Another advantage of cast iron is its low expansion with temperature. The surfaces of pistons were machined at a super-finish quality by grinding and polishing. The inner surfaces of the cylinder-liners are also treated at super-finish quality by honing and lapping. A 0.02 mm working clearance was left between pistons and cylinders, and no rings were used. A check-valve, which functions at very small pressure differences, was used to compensate the leaking gas through the gap between pistons and cylinders. The check-valve receives the air from the atmosphere while experiments are carried out at atmospheric charge pressure. In the case of high-pressure experiments, the check-valve receives the air from the pressurised workshop air system. A pressure reducer valve regulated the pressure of the inlet air.

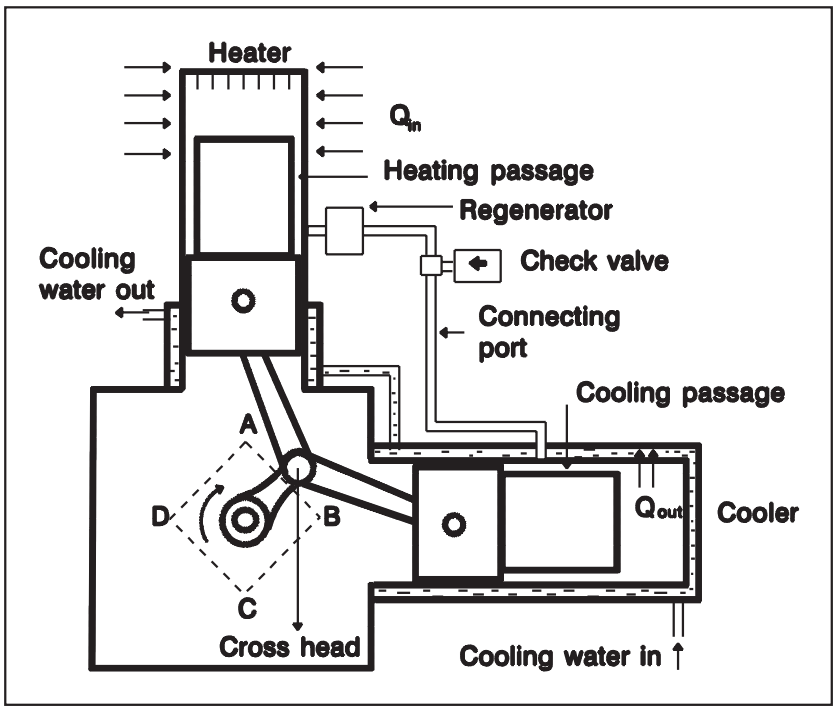

Figure 1. Schematic view of the test engine.

The heater consisted of heater head and a piston dome adjusted to the piston as seen in Figure 1. The process of heating was realised when the working gas flowed through the gap between the dome and heater head. In order to keep the cold head at low temperature, a water jacket was added to its outer surface.

The regenerator was constructed by staking a number of 100 M Chrome-Nickel woven wire gauzes at 70% porosity. One end of the regenerator was connected to the heater and the other end was connected to the cooler with a connecting pipe. The technical features of the test engine are shown in Table 1.

As is known, the theoretical Stirling cycle consists of two constant volume and two constant temperature processes. These processes can be explained as follows (Figure 1):

Figure 2. The crankshaft, piston rods and pistons assembly.

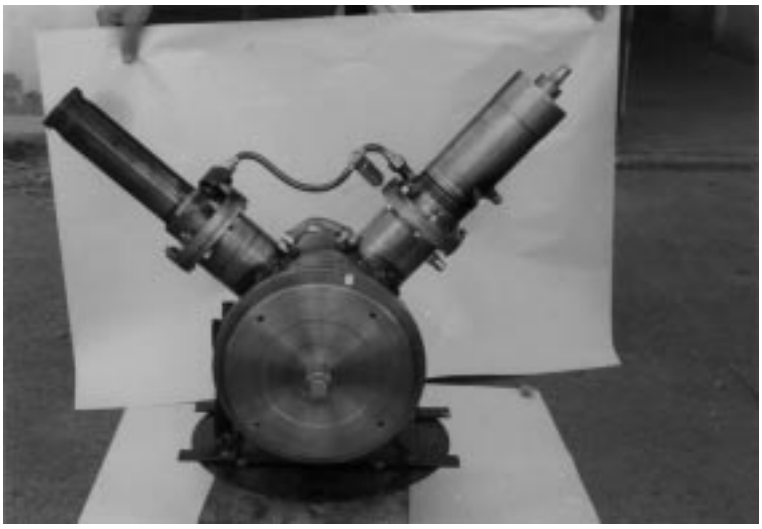

Figure 3. The test engine.

As the crosshead is at A, the hot piston is at the top of its stroke and the cold piston is at the middle of its stroke. When the crosshead moves from A to B, the hot piston moves downward and the cold piston moves upward. Consequently, the working gas at the volume above the cold piston flows to the volume above the hot piston, through the cooler, regenerator and heater. During this process, the sum of volumes above the cold and hot pistons is constant; therefore, this is a constant volume heating process. During this process, the gas passes through the cooler without heat exchange. Through the regenerator, however, a certain amount of heat exchange occurs. Through the hot passage between hot piston dome and heater head, the temperature of working gas increases to its maximum value. When the crosshead moves from B to C, both hot and cold pistons move downward and the expansion period is realised. As the working gas in the hot volume expands, some heat is transferred from the hot surface to the working gas and so the working gas temperature is kept constant. Unfortunately, during this process, some of the working gas returns to the cold volume due to expansion. During the motion of the crosshead from C to D, the cold piston continues to move downward and the hot piston moves upward. The working gas flows from the hot cylinder to the cold cylinder over the heater, regenerator and cooler. Since the increase

in volume of the cold cylinder and the decrease in the hot cylinder are equal, this is a constant volume process. Through the heater, there is no heat transfer to the working gas. Through the regenerator, due to heat transfer from the working gas to the matrix, the temperature of the working gas decreases partially. The rest of the heat of the working gas is rejected to the cooler. During the motion of the crosshead from D to A, both pistons move upward. At the end of this period, the cold piston reaches the middle of its stroke and the hot piston reaches the top of its stroke, compressing working gas at a constant temperature, and the cycle is completed. During the last process, the working gas gives its excess energy to the cooling water.

Table 1. Technical features of the test engine.

Engine type	α (V)
Cylinder bore	52.4 mm
Cylinder stroke	60 mm
Swept volume	129.39 cm^3
Phase angle	90 °
Heater dead volume	53 cm^3
Cooler dead volume	43 cm^3
Regenerator dead volume	12 cm^3
Total dead volume	108 cm^3
Working gas	Air
Max. engine speed	850 rpm
Max. engine power	65 W at 555 rpm
Cooling	Water
Total heater area	343 cm^2
Total cooler area	299 cm^2
Compression ratio	1.8:1

Experimental Procedure

The aim of this work was to determine the engine torque under various working conditions. Heat was supplied by an electrical furnace capable of producing up to 1500±5°C. The heater of the engine was inserted into the furnace through a window opened on its wall. Since the temperature in the furnace during the experiment was above 600°C, the heat transfer from the furnace to the heater head of the engine was expected to be predominantly by radiation, and no heat transfer resistance was present on the external surface of the heater head. The temperatures of the heater head and the furnace were assumed to be the same since the furnace was able to produce much more heat than the engine extracted. Tap water (at 20°C) was circulated with a flow rate sufficient to extract the excess heat in the cooling system of the engine.

In order to determine the performance characteristics of the engine, torque was measured versus speed. The measurement of engine speed was made by digital photo tachometer with 1 rpm precision. A Prony type dynamometer with 1 gr precision was used for measuring the torque. Initially, the furnace was set to a predetermined temperature. After reaching the desired temperature, the first test was carried out at ambient pressure and then the pressure increased to the other stages gradually. The furnace temperature was increased to the next level, and at this temperature tests were repeated at all pressure stages.

By continuing the same operations, the pressure varied from 1 bar to 4 bars with a 0.5 bars increase, and the furnace temperature varied from 600°C to 1100°C with an increase of 50°C. At each experimental condition, as much as possible data was recorded. Data obtained were converted to graphics and presented below.

Results and Discussion

The engine begins to run at about 500°C furnace temperature. The torque of the engine can be measured above 600°C furnace temperature. At a furnace temperature of 600°C, the maximum torque

and power were measured at ambient and found to be 0.3 Nm and 6.2 W respectively. At a furnace temperature of 700°C, the torque and power increased to 0.4 Nm and 8 W respectively. For a furnace temperature below 750°C, the charge pressure had a negative effect on the torque and power. As the furnace temperature was constant at 600°C, the increase of charge pressure from ambient condition to 0.5 bars caused the engine to stop. At a furnace temperature of 700°C, the same condition due to the charge pressure did not cause the engine to stop, instead causing a decrease in torque. A furnace temperature of about 600-750°C was adequate to heat the mass of working gas corresponding to the ambient pressure. When the mass of working gas in the engine was increased, the temperature of the gas became lower compared to the ambient pressure. For this reason, below a furnace temperature of 750°C the charge pressure shows negative effect. It is also plausible that in the experimental engine the working gas is charged only into the working space and a pressure difference occurs between working space and crankcase. This pressure difference may have increased the leakage of working gas and reduced the power.

The variation of power with charge pressure is shown in Figure 4 for T≥750°C. At each furnace temperature, the charge pressure has an optimum value. For a hot source temperature of 750°C, the optimum charge pressure can be seen around 1.5-2 bars. With a higher charge pressure, due to the reasons mentioned earlier, the power decreased. The difference of powers measured at 1 and 2 bars charge pressure was about 2 W for a furnace temperature of 750°C. When the furnace temperature increased to 1100°C, the optimum charge pressure appeared as 2.5 bars.

The maximum engine power is seen in Figure 5 as a function of furnace temperature. The power curve obtained at ambient pressure differs from the curves obtained for higher charge pressures. At ambient pressure, the increase of power with furnace temperature terminates after 900°C. At higher charge pressures, however, power shows a considerable increase. As the hot source temperature of Stirling cycle engines increases, the efficiency approaches 100% and the cyclic heat transfer to working gas increases. Therefore, within the temperature range of the experiments, a sharp increase in power is expected. The exceptional situation at ambient pressure is probably caused by some mechanical reasons and gas leakage.

Figure 6 shows the variation of torque with speed at 900°C including different charge pressures. As the speed decreases, the heating and cooling periods of working gas become larger and consequently the torque increases. At all furnace temperatures and charge pressures the torque shows similar variation with speed.

Figure 7 shows the variation of engine power with speed at a constant furnace temperature of 1100°C and different charge pressures ranging from 1 to 4 bars. At each pressure level, the power curves versus speed show similar behaviour. The variation of power with speed resembles that of internal combustion engines. At a certain speed, the power reaches a maximum value. Since the power is a function of speed and torque the lower the speed and torque, the less the power. The decline of power after a certain speed is attributed to inadequate heat transfer. In Figure 7 it is seen that the power curves obtained at charge pressures of 3 and 4 bars are below the curve obtained at 2.5 bars. Therefore, the optimum charge pressure is 2.5 bars for this engine in the present operating conditions. Under these conditions, the maximum engine power obtained was about 65 W at 555 rpm.

Figure 8 shows the variation of power with engine speed at optimum charge pressure, which is 2.5 bars, and at different hot source temperatures. It was observed that as the temperature increased, the power also increased.

In this experimental work, the power of the engine showed less power than the theoretical prediction carried out by Karabulut (1998). This difference may be related to the insufficient heat transfer through the inner surface of the heater to the working gas due to convective heat transfer resistance. The experimental results given in Figures 4-8 were obtained with an internally finned heater having 100cm^2 extra surface. The experiments carried out with a heater having no inner fins give 12% less power at 1100°C furnace temperature and 2.5 bars charge pressure.

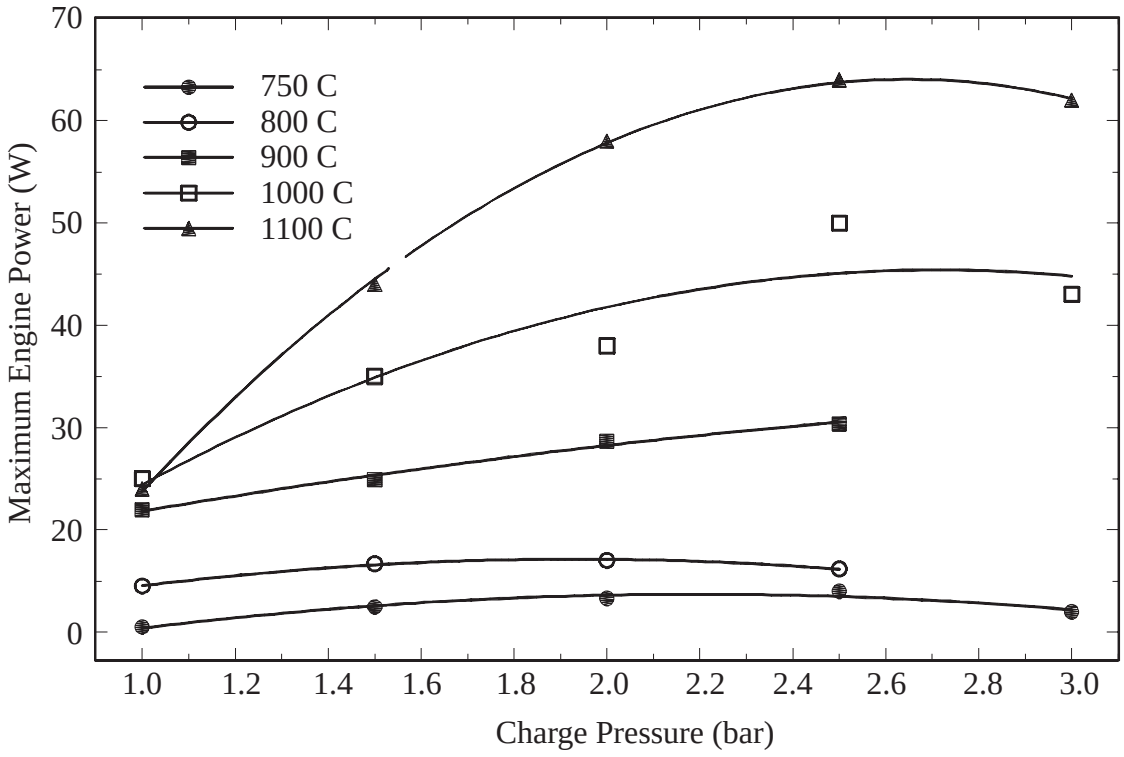

Figure 4. Variation of power with charge pressure at different hot source temperatures.

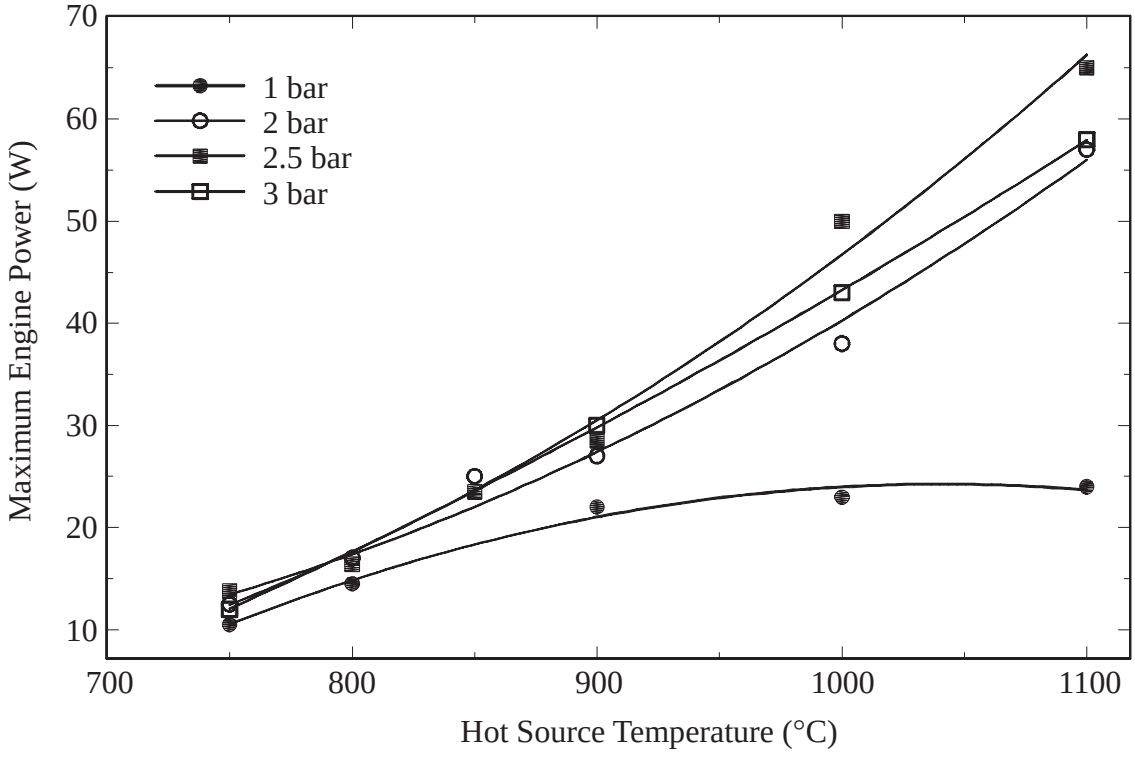

Figure 5. Variation of power with hot source temperature at different constant charge pressures.

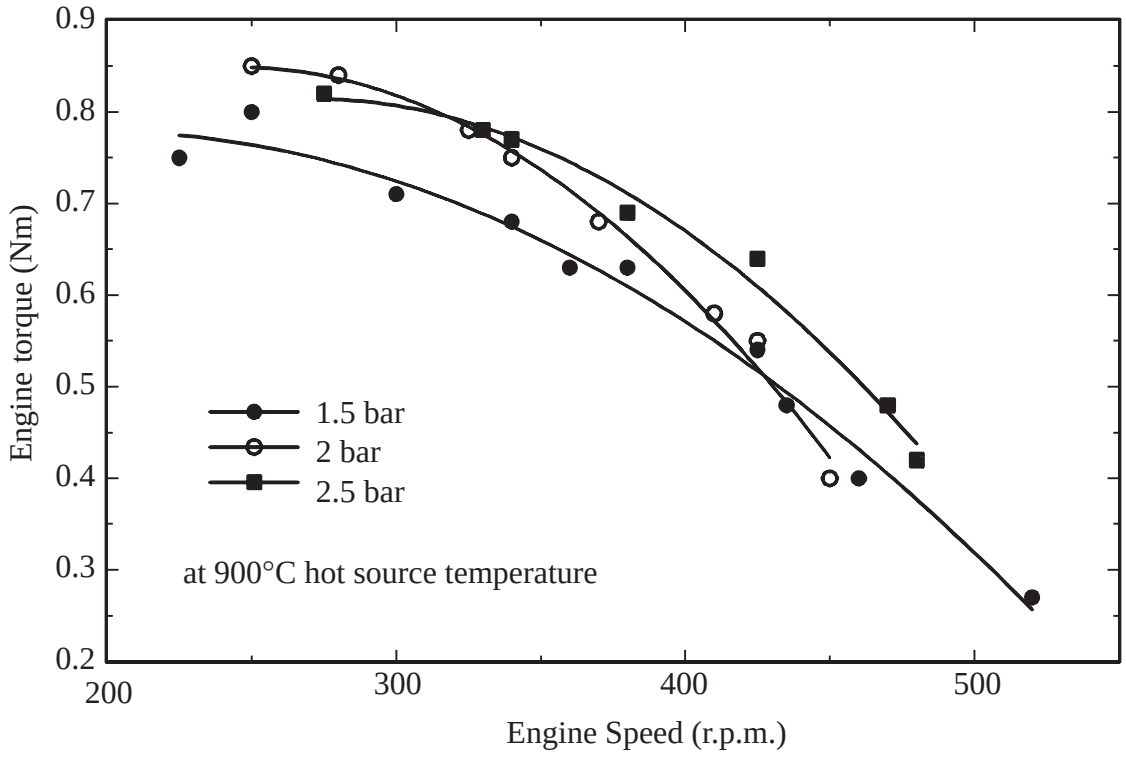

Figure 6. Variation engine torque with engine speed at 900°C hot source temperature and different charge pressure.

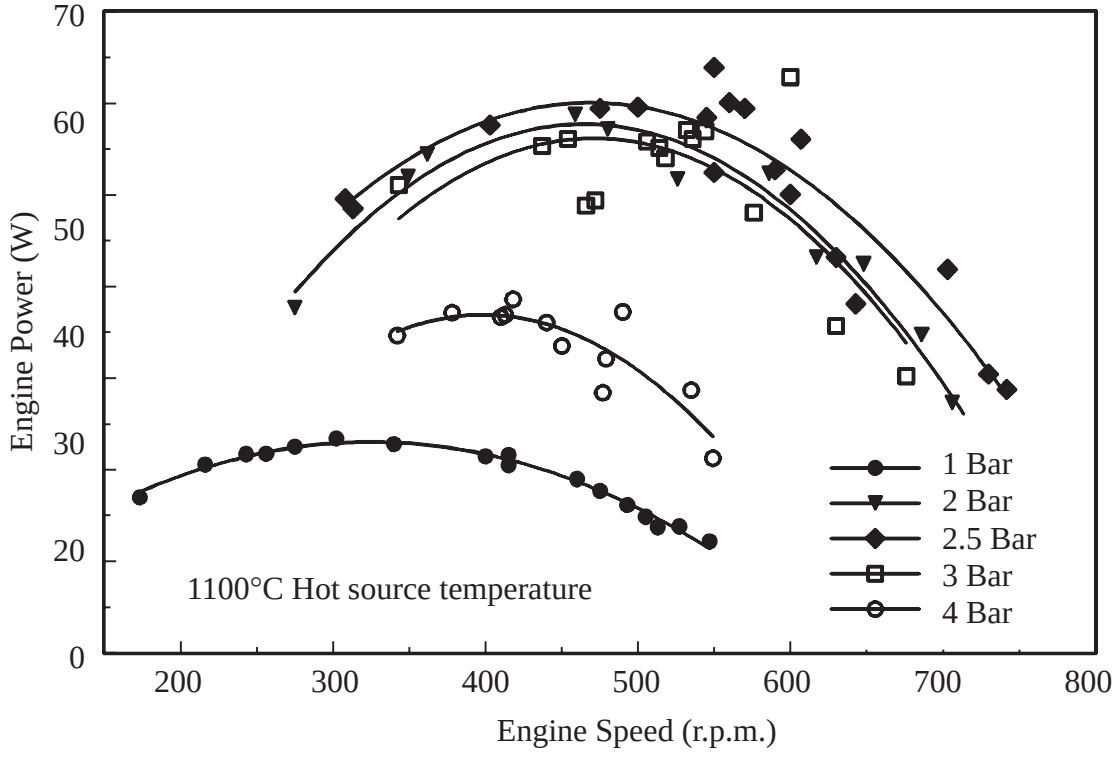

Figure 7. Variation of engine power with engine speed at 1100°C hot source temperature and different charge pressures.

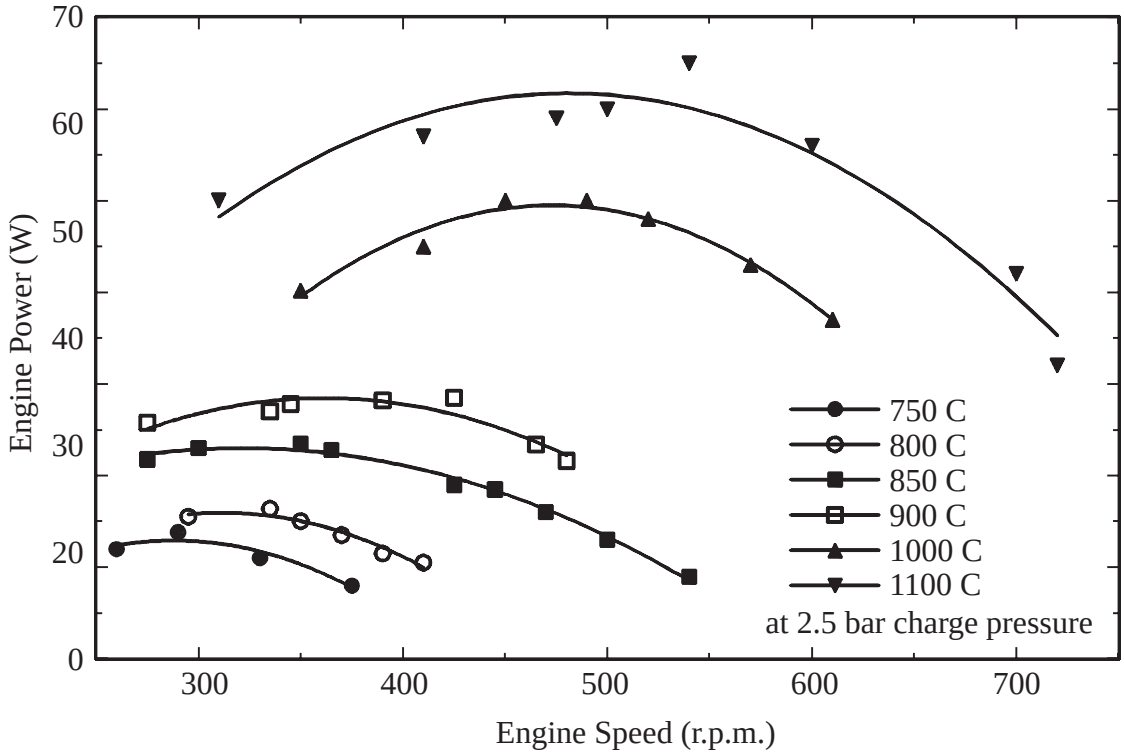

Figure 8. Variation engine power with engine speed at optimum charge pressure and different hot source temperatures.

Conclusion

This experimental work revealed that leakage of working gas has a significant effect on the performance of Stirling engines. The leak of working gas per cycle from working space to crankcase increases due to the pressure difference between the working space and crankcase caused by the charging of working gas into the working space. In order to prevent the leak of working gas from the working space to the crankcase, the gas should be charged into the crankcase instead of into the working space.

In order to be able to improve the performance of Stirling engines, a higher heater temperature is needed. Thus better temperature-resistant materials are required. In addition, by the enlargement of the inner surface of the heater, the power of the engine can be increased. It is also necessary to improve the convection heat transfer coefficient of the heater inner surface. This can be clarified by investigating different surface shapes instead of the smooth surface. Cast iron pistons without rings, which require no regular lubrication, have been used successfully.

References

Beale, W., Holmes, W., Lewis, S., and Cheng, E., "Free-Piston Stirling Engine-A Progress Report", SAE, Paper no: 730647, 1973.

Finkelstein, T., "Air Engines II", The Engineer, April 3, 522-527, 1959a.

Finkelstein, T., "Air Engines III", The Engineer, April 10, 568-571, 1959b.

Finkelstein, T., "Air Engines IV" , The Engineer, May 8, 720-723, 1959c.

Finkelstein, T., "Thermodynamic Analysis of Stirling Engines", Journal of Spacecraft and Rockets, 4, No-9, 1184-1189, September 1967.

Karabulut, H. "Stirling Motorlarının Termodinamik Similasyonu"', Isı Bilimi ve Tekniği Dergisi, 19, Sayı 1-2, 21-25, 1998.

Meijer, R. J., "The Philips Stirling Thermal Engine", Thesis, Technische Hogeschool Delft, November 1960.

Michels, A. P. J., "The Philips Stirling Engine: A Study its Efficiency As a Function of Operating Temperatures and Working Fluids", 769258, 11 th IECEC, Sahara Tahoe Hotel, Statline, Nevada, September 12-17, 1976.

Rix, D. H., "Some Aspects of the Outline Design Specification of a 0.5 kW Stirling Engine for Domestic Scale Co-generation", Journal of Power and Energy, IMechE, 210, 25-33, 1996.

Schimidt, G., "The Theory of Lehmanns Calorimetric Machine", Zeitschrift des Vereines Deutcher Ingenieure, 15, Part 1. Jan 1871.

Tew, R., Jefferies, K., and Miao, D., "A Stirling Engine Computer Model for Performance Calculations", Report no: DOE/NASA/1011-78/24, July 1978.

Urieli, I. and Rallis, C. J., "Stirling Cycle Engine Development-A Review" Energy Utilization Unit, Paper No: 7-5, University of Cape Town, 1975.

Urielli, I., Kushnir, M., "The Ideal Adiabatic Cycle - A Rational Basis For Stirling Engine Analysis", 17th IECEC, Westin Bonaventure, Los Angles, California, 8-12 August 1982.

Urieli, U., Berchowitz, D. M., 1967, "Stirling Cycle Machine Analysis", Adam Hilger Ltd., Bristol, 1984.

Walker, G., "Stirling Engines", Claredon Press, Oxford, 1981.